METEOROLOGICAL APPLICATIONS
Meteorol. Appl. **17**: 433–441 (2010)
Published online 22 February 2010 in Wiley Online Library
(wileyonlinelibrary.com) DOI: 10.1002/met.175

A seasonal forecast scheme for spring dust storm predictions in Northern China

Tao Gao,[a]* Zhang Xuebin[b] and Wulan [a]

[a] *Inner Mongolia Meteorological Institute, Hohhot 010051, Inner Mongolia, P. R. of China*
[b] *Climate Research Division, Science and Technology Branch, Environment Canada, ON, M3H 5T4, Canada*

ABSTRACT: The theme discussed in the present study is that of spring dust storm seasonal forecasts in Northern China. A comprehensive investigation of observations collected from 65 stations in Northern China, which studied strong winds for 35 years (1971–2005) and dust storms for 48 years (1961–2008), concluded that strong winds, which are recognized as a crucially dynamic factor, have unsurprisingly proven to be strongly related to dust storm activity. Therefore, determining effective predictors for strong winds should be helpful in spring dust storm forecasts. By employing this idea, comprehensive correlation analyses among the strong winds, dust storms and other influential elements from the oceans and the atmospheric circulations can be seen. From the spatial correlation fields between prior sea surface temperatures and the strong winds, four regions with higher oceanic coefficiencies are confirmed. The method of EOF (Empirical Orthogonal Function) decomposition is adopted to extract forecast signals from prior precipitation in Northern China and sea surface temperatures of those regions. The multivariable step-regression model is employed to select efficient predictors and the multivariable regression model is used to create forecast equations. With the cross validation approach, six series of 48 year hindcasts with six different predictor sets are conducted. Furthermore, the three-classification forecast method is used to judge successful or failed dust storm forecasts. Together, forecast skills of probability of detection and skill score suggest that series forecasts are better than random forecasts. The best forecast skill is gained from using the predictor set selected by the multivariable step-regression model. Copyright © 2010 Royal Meteorological Society

KEY WORDS dust storms; Northern China; spring seasonal forecast; forecast signals; predictors; hindcasts

Received 5 February 2009; Revised 11 September 2009; Accepted 30 October 2009

1. Introduction

Dust storms are the type of natural disaster which is most likely to occur in arid and semiarid regions in the world, such as central and eastern Asia, the Sahara Desert and some regions in Australia, North America and elsewhere. It is believed that there are two major factors which influence dust storm formation: one is the surface conditions which have been identified to play an important role in sand and dust material source in the deserts and poorly vegetated areas in East Asia (Shi *et al*., 2000; Liu *et al*., 2003; Liu *et al*., 2004): however, the one and only critical element, which is recognized as a crucially dynamic factor in the formation of dust storms is strong winds (Kurosaki and Mikami, 2003; Zhang *et al*., 2005a). Most of the dust storms in East Asia are related to the outbreaks of North Polar cold air in springs and winters. These outbreaks, in general, yield strong wind, which is the major phenomenon of cyclone activity in the medium-high latitude zone in the Northern Hemisphere (Qian *et al*., 2002). In recent years, upon the consideration of different regions or study purposes, many research efforts focus on dust storm monitoring by using different observation equipment, such as satellite, lidar apparatus, observing instruments for measuring total suspending particle (TSP), particulate matter 10 μm in aerodynamic diameter (PM_{10}) or smaller, $PM_{2.5}$, and even $PM_{1.0}$ (Miller, 2003; Chung *et al*., 2005; Yasui *et al*., 2005; Zhang *et al*., 2005b). In addition, some other referential studies concentrate on fields such as: the synoptic situation and atmospheric circulation analyses, particular dust storm events or processes dynamic diagnoses (Yang *et al*., 2008), synthesis of temporal-spatial characteristics of regional dust storms, analyses of dust storm moving paths and sand-dust particle transportation and deposition (Gong *et al*., 2006). Other studies have focused on areas such as: evaluation of the impacts of climate change on dust storms (Qian *et al*., 2002), anthropogenic influence, air pollution, and influence on human health related to dust storms (Liu *et al*., 2006), identification of the correlations between surface conditions and dust storms (Zou and Zhai, 2004), and establishment of forecast schemes for short-term dust storm weather predictions based on coupled numerical forecast models, satellite images, meteorological observations and synoptic chart analysis (Gao *et al*., 2002; Shao *et al*., 2003; Hu *et al*., 2008; Wang *et al*., 2008;). Also, there has been an

* Correspondence to: Tao Gao, Inner Mongolia Meteorological Institute, Hohhot 010051, Inner Mongolia, P. R. of China.
E-mail: Frautao@yahoo.com

artificial neural network applied in short-term dust storm forecast by employing a combination of daily mean meteorological measurements (Huang *et al*., 2006).

Aimed at establishing a spring season dust storm forecast scheme for Northern China, the multivariable step-regression model is used to select main effective predictors in setting up predictor sets for forecast equations. Forecast equations used in 48 year (1961–2008) hindcast experiments are established by using the multivariable regression model. The cross validation method is followed in the selection of the best predictor set and hindcast experiments, and the three-classification distinguishing scheme is used to judge success or failure forecasts in dust storm frequencies. It can be learnt from verifying the forecast skill of probability of detection (POD) and skill score (SS) that both the POD and SS of the seasonal prediction scheme are better than those of the random forecasts.

2. Data, definitions and methods

2.1. Data

The available four daily surface meteorological observations (after data quality checked) including horizontal visibility, wind velocity and precipitation observed at 65 stations in the domain (at 0000, 0600, 1200 and 1800 UTC) are employed for compiling datasets of dust storm events (DSEs), severe dust storm events (SDSEs) and strong wind events (SWEs), which were obtained from the Meteorological Data Service Centre of China Meteorological Administration (CMA). The global $5^\circ \times 5^\circ$ grid monthly sea surface temperature anomalies (SSTA) are downloaded from the website of the Climate Research Unit (CRU), UK (http://www.cru.uea.ac.uk/cru/data/). The atmospheric circulation indices are released by Beijing Climate Centre of the CMA.

2.2. Definitions

Specific defining difference between a dust storm day and a dust storm event, is the most fundamental issue in dust storm studies. In one aspect, although the definition of suspended dust weather, a dust storm day, a severe dust storm day, or a strong dust storm day, is usually identified by a single observation station, it should be noted that a dust storm day, as defined by Fang *et al*. (1993) is a day in which horizontal visibility is observed to be below 1000 m. There is, however, still no commonly recognized definition for DSEs or SDSEs. A dust storm event may include several stations with dust storm records (observed horizontal visibility is below 1000 m) and it may live more than 1 day with a cold air attacking process.

In the present study, the frequency sequences of the DSEs, SDSEs and SWEs are derived from the calculations in comprehensive investigations at 65 meteorological stations in the domain (35–45°N, 94–120°E), which mainly include the middle and Western parts of Inner Mongolia, Northwestern Gansu Province, Ningxia Hui Autonomous Region and the Northern part of Shannxi Province (Figure 1). A score is to be given to a station with a dust storm or a severe dust storm record if the observed horizontal visibility is below 1000 or 500 m among daily observations at the four regular times (0000, 0600, 1200 and 1800 UTC). According to the total number of the scored stations in all 65 observatories in the domain, DSE, SDSE and SWE are specifically defined in Table I. By using a Geographic Information System (GIS) as a calculation tool, the core influence areas of the DSEs, SDSEs and SWEs are estimated within the

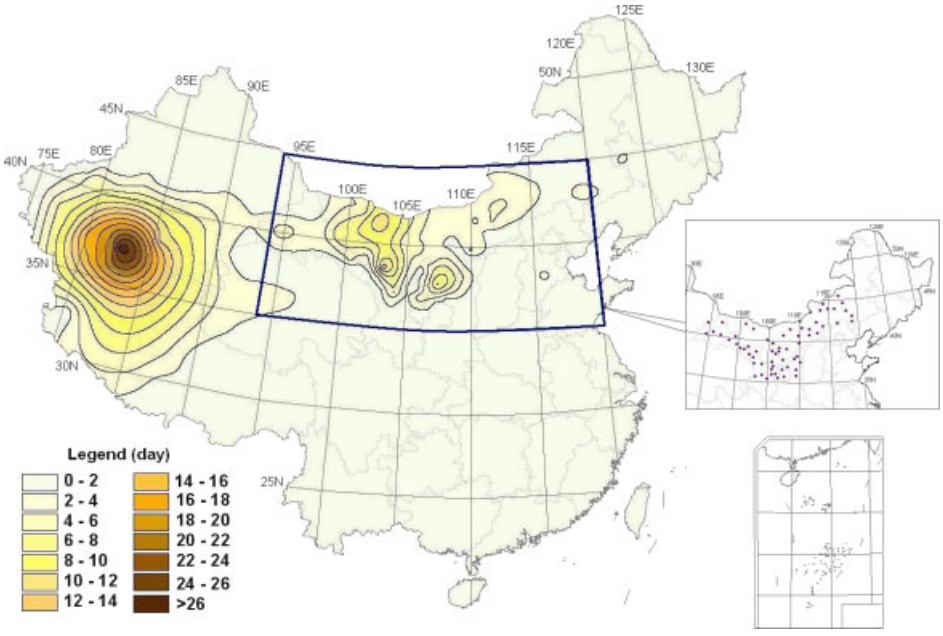

Figure 1. Mean spring dust storm distributions of China (1961–2005), studied domain (rectangle region) and locations of the 65 observation stations in Northern China. This figure is available in colour online at wileyonlinelibrary.com/journal/met

circle drawn from the five nearest stations among the 65 stations in the domain. The highest daily wind speed is attained from the records of automatic wind speed instruments. A single station with strong wind score is defined if the highest wind velocity in a day equals to or over 17 m s^{-1}. Here, a dust storm event or a strong wind event may last 1, 2 or even several days.

2.3. Methods

The EOF decomposition method is used to extract signals from previous monthly sea surface temperatures of the oceans and the monthly precipitations measured at the 65 stations. Two steps are followed to select predictor groups to fit the forecast model. First, some influence factors from a large number of elements of the oceans and the atmospheric circulations are primarily chosen by means of correlation analysis. The multivariable step-regression model is employed in the second step to confirm the best predictor set from those factors initially selected in the first step. In the second step, the cross validation is used in the selection of the best predictor set with the target forecast year excluded in model fitting for each year (von Storch and Zwiers, 1999). The most common predictor groups with the smallest number of those factors left in the final step of the multivariable step-regression model for each year are then selected. The forecast equations used in the hindcast experiments are set up by using the multivariable regression model. Hindcast experiments are conducted by following the cross validation, in which each forecast year sample was withheld from the data base when building a regression equation to forecast this target year.

2.4. Forecast skill

To quantify and appraise forecast skill, the probability of detection (POD) is computed, the ratio of correct forecast to the number of times the particular event occurred, thereby giving us an indicator of forecast skill of the predictors. The POD is defined as follows (Wilks, 1995):

$$POD = \frac{a}{a+c} \tag{1}$$

In the above equation, a is the number of observations that occurred and forecasts issued, and c is the number of observation occurred but were not predicted. This POD has a value range from 0 to 1. A zero value for the POD means no quantifiable forecast skill, and one indicates a perfect forecast. Three categorical forecasts of discrete predictions are used in the hindcasts (Wilks, 1995). The POD is computed according to the contingency table for three dust storm frequencies sorted as below-, near- and above-normal frequencies. The tercile boundaries are determined by ranking the samples of the 48 year frequencies (1961–2008), each class respectively containing the frequencies of 16 samples (Table II). Since each of the three classifications has the same occurrence probability, a forecast purely by random gives 0.240 in the POD. That is to say, the POD needs to be larger than this value for the predictors to be useful in predicting a particular category of dust storm frequencies.

A kind of skill score (SS) is also used to evaluate potential forecast skill. The SS for forecasts characterized by a particular measure of accuracy of A, with respect to the accuracy A_{ref} of a set of reference forecasts, takes the following form (Wilks, 1995):

$$SS = \frac{A - A_{\text{ref}}}{A_{\text{perf}} - A_{\text{ref}}} \times 100\% \tag{2}$$

Here, A_{perf} represents the value of the accuracy measure that would be achieved by perfect forecasts and A_{ref} is determined by using climatological forecasts as reference forecasts, given by Yan (2003):

$$A_{\text{ref}} = \sum_{i=1}^{I} F_i \times A_i \tag{3}$$

For this equation, I represents forecast categories, F_i is climatological probabilities and A_i forecast times. SS equals 100% for perfect forecasts and 0% if there is no improvement over the reference forecasts. It is greater (less) than 0% if the forecasts are superior (inferior) to the reference forecasts.

Table I. Definition of the dust storm event (DSE), severe dust storm event (SDSE), strong wind event (SWE) and core influence areas.

Element	Total number of stations on the worst day	Horizontal visibility (m) and wind speed (m s^{-1})	Estimated core influence areas (km^2)
DSE	≥5	≤1000 m	≥19805.8
SDSE	≥5	≤500 m	≥19805.8
SWE	≥5	≥17	≥19805.8

Table II. Dust storm frequency intervals of the three-classification forecast scheme.

Frequency interval	Dust storm events	Severe dust storm events
Below normal	[0, 3]	[0, 1]
Normal	[4, 7]	[2, 4]
Above normal	[8,∞]	[5, ∞]

3. Selecting of predictors

Two major dust storm source regions in East Asia are confirmed in some researches. One is the areas of the Taklimakan Desert and the other is the region including Mongolia and the Northern China (Sun *et al.*, 2001). Furthermore, two areas frequently attacked by dust storms can be clearly recognized from the spatial distribution of the dust storms in China (Figure 1). It has been demonstrated that the dust storms which

occurred in the domain are more directly influential than the others to the downwind regions, such as Beijing-Tianjin Region, the Korean Peninsula and Japan (Sun *et al*., 2001; Gao *et al*., 2006). According to statistical calculations, a significant declining trend of dust storm events can be seen during 1961–2008 in Northern China (Figure 2). Moreover, it can also be learnt from Figure 3 that spring (March–May) is the most frequent dust storm season in a year. Nevertheless, some SDSEs still might break out in February, June, or in winter months. For instance, a severe dust storm event occurred 1–2 June 1961 with 18 stations recording below 500 m horizontal visibilities on the worst day and another attacked the region 19–21 February 1977, in which five stations in the domain observed visibilities below 500 m on the worst day. Due to these, a longer period is considered in this study, which starts from the first day of February and ends the last day of June. This longer period is still referred to as 'springtime' in this paper. As a note on strong winds in relation to dust storm frequency, it is indicated in Xu's study (Xu *et al*., 2006) that the surface wind speed of East Asia has significantly declined since late 1960s with weakening winter monsoons.

Outcomes of the statistical analyses in this study reveal a strong positive correlation between DSEs to SWEs, as well as SDSEs to SWEs. The same trends of the SDSEs and SWEs can be seen in Figure 4, which means that the phenomena of the decreasing tendency of dust storm occurrences were accompanied by a declining trend of strong wind event frequencies during the past several decades in Northern China. A close correlation between dust storms and the SWEs is identified, even after the linear trend was removed from both of the original frequency series (Table III).

Correlations between SWEs to the atmospheric circulation indices (ACIs), DSEs to ACIs and SDSEs to ACIs indicate that some of them presented significant forecast signals in the previous periods. The information and explanation of the primarily selected influence elements are listed in Table IV.

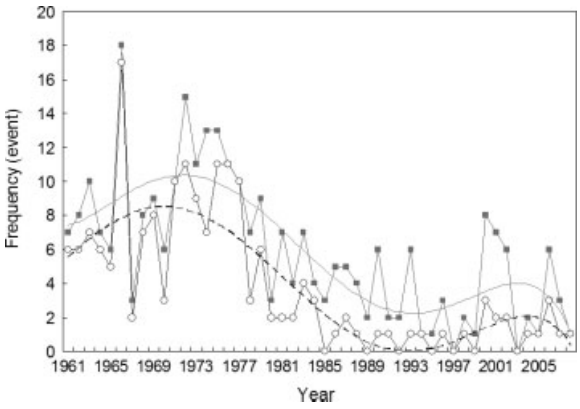

Figure 2. Inter-annual frequency variations of spring dust storm events (solid line with filled squares) and trend (solid line), severe dust storm events (solid line with hollow circles) and trend (dashed line) of Northern China during 1961–2008.

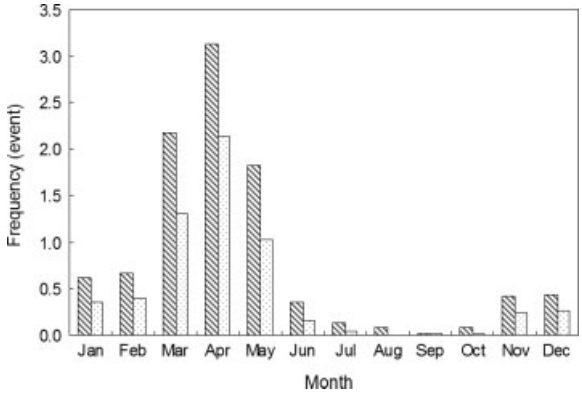

Figure 3. Mean monthly frequencies of dust storm (backslashed bars) and severe dust storm events (dotted bars) of Northern China (1961–2008).

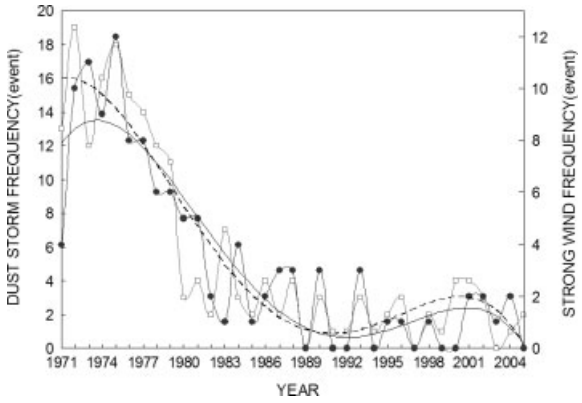

Figure 4. Variations of strong wind events (soled line with filled circles) and trend (solid line), severe dust storm events (solid line with hollow squares) and trend (dashed line) of Northern China during spring times from 1971 to 2005.

Table III. Correlation coefficients between spring dust storms and strong wind events of Northern China.

Coefficient (35a)	Dust storms	Strong wind events
Before linear trend removed	DSE	0.84
	SDSE	0.85
After linear trend removed	DSE	0.63
	SDSE	0.64

All coefficients are at 0.01 significance levels. SDE means dust storm events and SDSE donates severe dust storm events. 35a indicates 35 years (from 1971 to 2005).

The EOF decomposition method is employed to extract forecast signals from the oceans. In the correlation field between previous SSTA and SWEs of 35 years (1971–2005), four sensitive regions with high coefficients can been found in Figure 5. Two of them are in the Pacific Ocean, named region 1 (50–60°N; 160°E–130°W) and region 2 (20°S–20°N; 140°E–110°W), and the other two, region 3 (EQ-45°N; 0–60°W) and region 4 (15°S–15°N; 60–110°E) are

Table IV. Explanation of primarily selected predictors.

Number	Predictor name	Explanation
1	R1-EOF-PC1	First principal component of the EOF of the monthly SSTA over the far northern Pacific Ocean (50–60°N, 160°E–130°W)
2	R2-EOF-PC1	First principal component of the EOF of the monthly SSTA over the tropical-subtropical Pacific Ocean (20°S–20°N, 140°E–110°W)
3	R3-EOF-PC1	First principal component of the EOF of the monthly SSTA over the North Atlantic Ocean (EQ-45°N,0–60°W)
4	R4-EOF-PC1	First principal component of the EOF of the monthly SSTA over the North India Ocean (15°S–15°N, 60–110°E)
5	65R%-EOF-PC1	First principal component of the EOF of monthly precipitation percentiles at 65 observation stations in northern China
6	AI of NHSH	Index of the area of the Northern hemisphere subtropical high (5°–355°E)
7	SI of NHSH	Index of the strength of the Northern hemisphere subtropical high (5°–355°E)
8	WEI of WPSH	Index of the western extend of subtropical high over the western Pacific
9	AI of NPV	Index of the area of the North hemisphere polar vortex (5°–355°E)
10	SI of NPV	Index of the strength of the North hemisphere polar vortex (5°–355°E)
11	SI of IBT	Index of the strength of the India-Burma trough (15–20°N, 80–100°E)

located in the Atlantic and India Oceans respectively (Figure 6). Relatively close correlations stand between the SWEs, DSEs, SDSEs in relation to the frequency sequences and the first coefficient series of the EOF leading principal component (EOF-PC1) of the prior SSTA over the four sensitive regions. The correlation coefficients and the EOF-PC1 explanations of the total variances are shown in Table V. In consideration of these facts, the EOF-PC1 of those sensitive regions can be included in the predictor set for model fitting in hindcast experiments.

From the correlation field between prior year precipitation and spring dust storms of China, a relative higher associated area can be found in the domain (Figure 7). The EOF decomposition method is employed to synthesize the signals of the preceding monthly precipitation at all 65 stations. The variance explanation of the first time series of the EOF-PC1 and its correlation with dust storm events are illustrated in Table V. Here, the EOF-PC1 of the precipitations is considered to denote some signals from the surface conditions.

After a comprehensive predictor selection procedure, 11 initially selected factors are obtained. Further selection is made by using the multivariable step-regression model in order to establish a more effective predictor set which contains the elements chosen from those 11 factors. For the DSEs, five predictors were identified, and four were confirmed for the SDSEs. The message of the predictor sets can be obtained from Table VI.

4. Hindcast experiments and forecast skills

Two kinds of spring dust storms (DSEs and SDSEs) are forecasted with six different predictor sets in six series of the 48 year hindcast experiments. Considering detecting the forecast effects of the sea surface temperatures, the first and fourth predictor sets only involve the signals from the four sensitive regions in the oceans. In addition, the second and fifth sets are designed to include 11

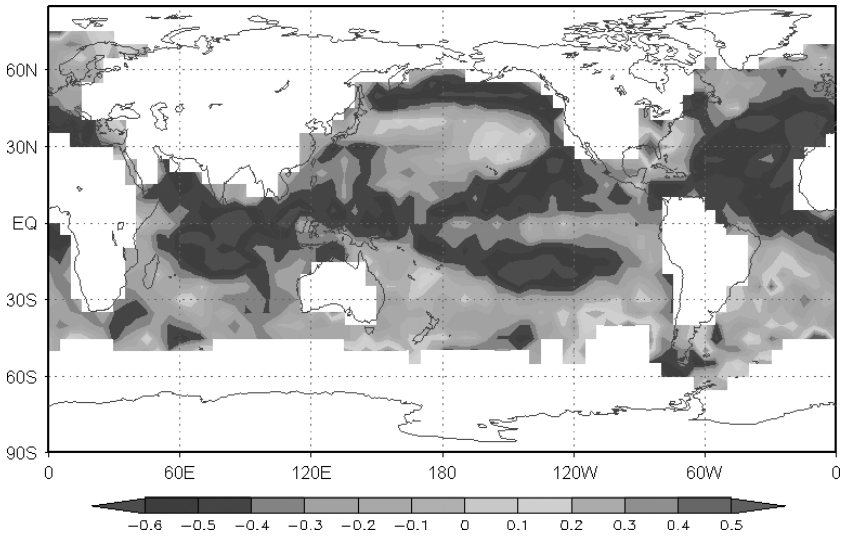

Figure 5. Correlation field between global sea surface temperature and strong wind events of Northern China (1971–2005).

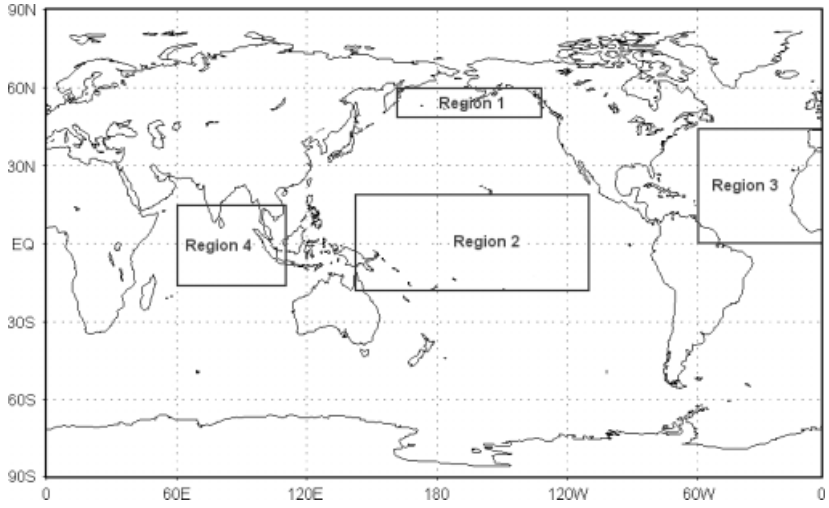

Figure 6. Four confirmed sensitive regions in the oceans.

primarily selected predictors, while the third and sixth sets merely use the predictors identified through the multivariable step-regression model.

Frequency intervals of the three dust storm categories are used to judge whether the forecast has succeeded or failed in the hindcasts. A forecast is recognized as having been successful if the predicted and observed frequencies of DSEs or SDSEs are in the same frequency interval in Table II. For example, both frequencies are in the interval of below normal and, if not, the forecast is determined to have failed.

The probability of detection (POD) values for the three dust storm categories is presented in Table VI. The entire POD of those categories is higher than that expected from random forecasts. That indicates the prior sea surface temperatures, antecedent years precipitation and some identified atmospheric circulation indices have certain degrees of influence in forecast skill for spring dust storm seasonal predictions. The skill scores (SS) for DSEs and SDSEs with different predictor sets are revealed in Table VII. All SS in the table are larger than one, which means that the predicting skills are superior to those of the climatological forecasts. In addition, the coefficients between forecasts and observations, listed in Table VII, and the scatter plot of observations *versus* forecasts, can been seen in Figure 8. All information from the POD, SS, coefficients and the scatter plot indicates that the primarily selected predictors are necessary in relation to forecasting skills to spring dust storms in Northern China. The state of previous sea surface temperatures performs helpful predicting signals, and the optimized predictor sets respectively for DSEs and SDSEs are the sets containing the climatic factors selected through the multivariable step-regression model. The results of hindcasts suggest that an efficient predictor set may yield an increasingly useful forecast skill for spring dust storm seasonal forecast in Northern China.

Table V. Correlation coefficients between the selected predictors and spring dust storms, selected predictors and spring strong winds.

Predictors	SWE (35)	DSE (48)	SDSE (48)	Variance explained (%)
R1-EOF-PC1 (pre-ann)	0.60	0.48	0.43	53.0
R2-EOF-PC1 (pre-ann)	0.44	0.51	0.46	29.6
R3-EOF-PC1 (pre-ann)	0.70	0.59	0.60	31.0
R4-EOF-PC1 (pre-ann)	0.65	0.46	0.51	32.4
65R%-EOF-PC1(pre-ann)	–	0.46*	0.45*	69.1
AI of NHSH(pre-sum)	−0.63	−0.72	−0.65	–
SI of NHSH(pre-sum)	−0.46	−0.65	−0.59	–
WEI of WPSH(pre-ann)	0.49	0.60	0.57	–
AI of NPV(pre-sum)	0.49	0.47	0.49	–
SI of NPV(pre-sum)	0.51	0.55	0.58	–
SI of IBT(pre-sum)	−0.72	−0.68	−0.57	–

Decoded signals of all acronyms in the left column can be seen in Table IV. All coefficients are at the 0.01 significance level except those with asterisk sign (*), which are at the 0.05 significance level. SDE means dust storm events, SDSE indicates severe dust storm events and SWE denotes strong wind events. 35 represents 35 years (SWE: 1971–2005; predictors: 1970–2004) and 48 denotes 48 years (dust storms: 1961–2008; predictors: 1960–2007). Pre-ann indicates the mean index value of the previous annual and pre-sum means the mean index value of the previous summer.

5. Summary and conclusions

In respect of the correlation analysis results, dust storms are strongly associated with SWEs in Northern China in springtime. There are four sensitive regions with higher correlation co-efficients to the SWEs in the oceans which are confirmed in the correlation field between SSTA to SWEs. The spring dust storms are associated with previous precipitation which denote some forecast signals from the surface conditions over the domain. In spite of this, some atmospheric circulation indices are shown to have relative close correlations with spring dust storms. It can be concluded from the outcomes of the 48 year hindcasts that the prior sea surface temperatures of the four sensitive regions displays efficient forecast signals

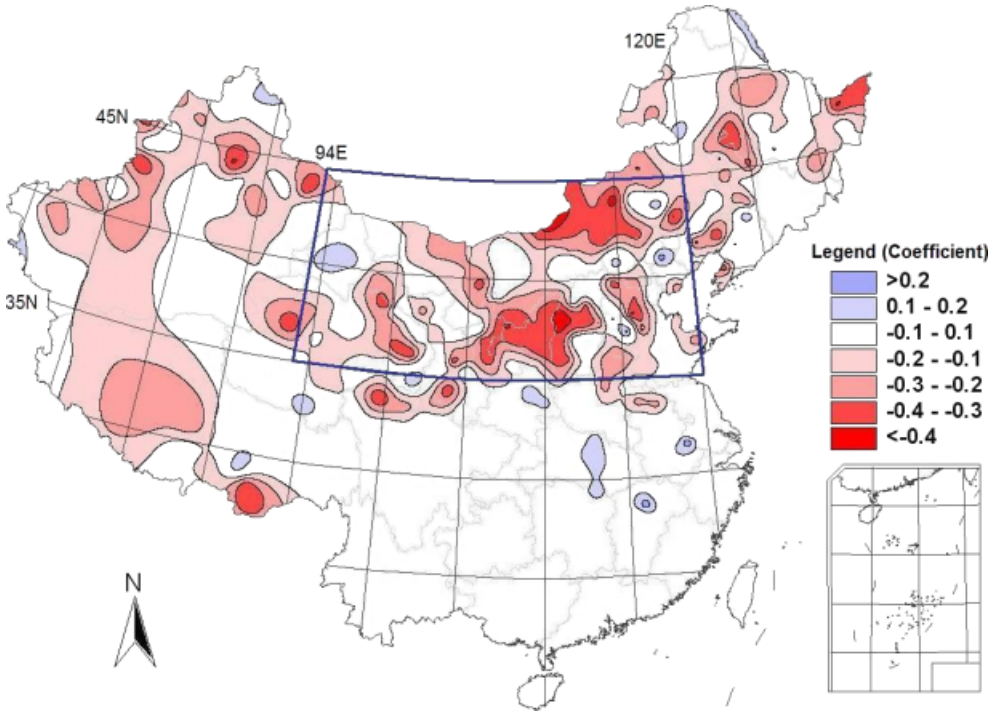

Figure 7. Correlation field between prior year precipitations and spring dust storms of China (1961–2005). This figure is available in colour online at wileyonlinelibrary.com/journal/met

Table VI. Probability of detection (POD).

	Dust storm events			Severe dust storm events		
Number of predictor set	1	2	3	4	5	6
Number of used predictors	1, 2, 3, 4	1–11	1, 2, 5, 10, 11	1, 2, 3, 4	1–11	1, 2, 4, 10
Below normal	0.417	0.647	0.647	0.450	0.500	0.813
Normal	0.529	0.765	0.824	0.450	0.417	0.813
Above normal	0.714	0.714	0.786	0.500	0.500	0.875

Following the predictor number in the third row, name of the used predictors can be seen in the second column of Table IV.

Table VII. Skill scores (SS) and averaged multiple correlation coefficients (R^2) of regression functions in the 48 year hindcasts.

Dust storm events			Severe dust storm events		
Number of predictor set	SS (%)	R^2	Number of predictor set	SS (%)	R^2
1	34.0	0.71	4	30.6	0.75
2	55.9	0.78	5	35.4	0.70
3	62.1	0.81	6	44.3	0.77

to dust storms in the coming springs. Positive forecast skills are demonstrated in the hindcast experiments by employing the multivariable regression model fitted with different predictor sets, which include factors such as: precipitation in previous years, the subtropical high of the Northern Hemisphere, the Western extension of the subtropical high over the Western Pacific, the strength of the India-Burma trough and the North Polar vortex. Both of the POD and SS suggest that the forecast skill is superior to that of the random forecasts.

Since the present study is mainly on the purpose of spring dust storm seasonal forecast in Northern China, the dynamic processes of those influence factors have not been put into consideration. Further researches are still necessary in investigations of the mechanical principles of the interactions among the dust storms, oceans, climate elements and atmospheric circulations.

Acknowledgements

The first author appreciates Mr. Ray P. Kenderdine and Miss Fountain Yu for helping in English improvement. Also many thanks are given to the anonymous reviewers and the editors for helpful comments and suggestions for revision of this article. This study is financed by National Natural Science Foundation of China (no. 40465001).

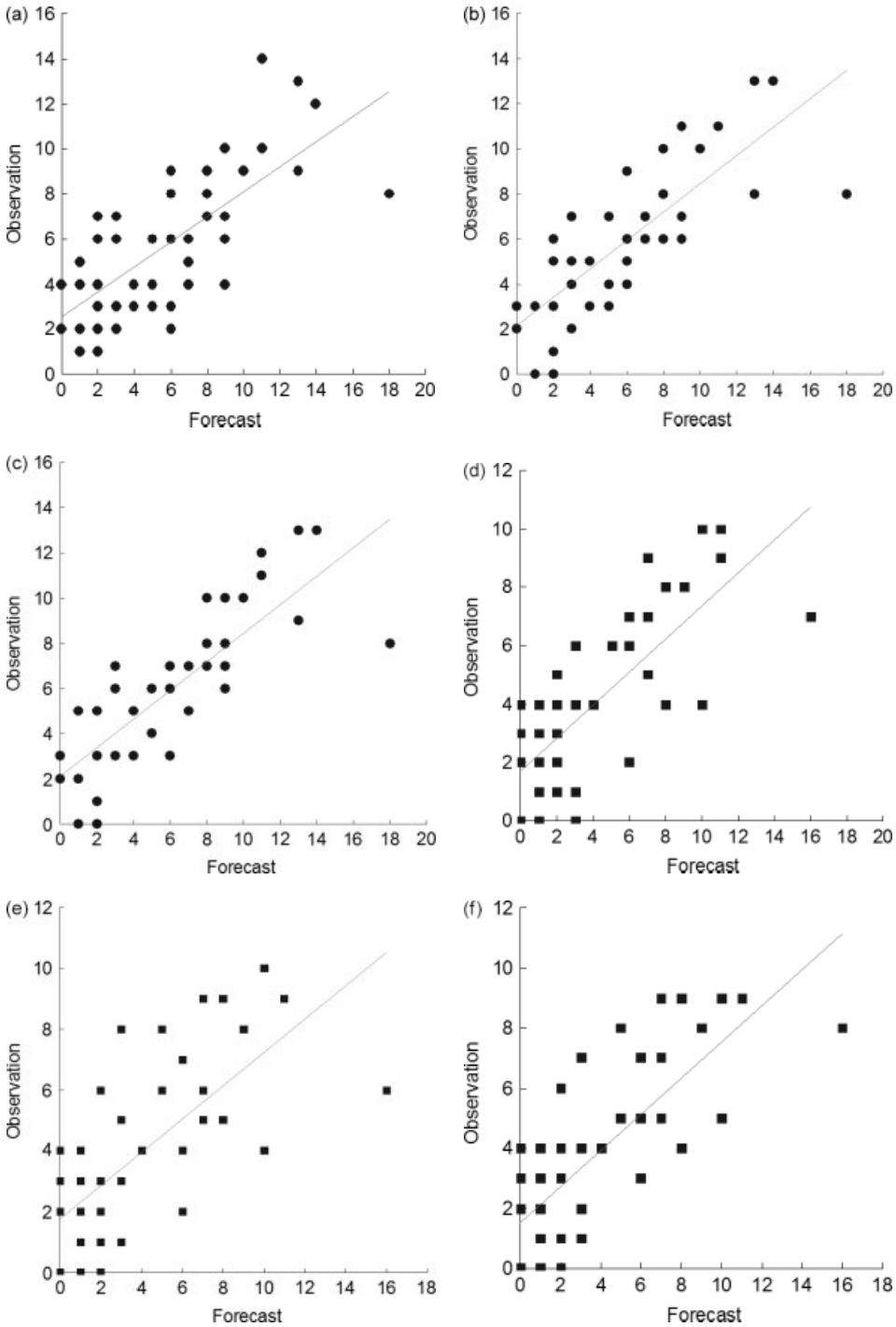

Figure 8. Scatter plot of observations versus forecasts. (a–c) for dust storm event forecast by using predictor set number 1, 2 and 3. (d–f) for severe dust storm event forecast by using predictor set number 4, 5 and 6.

References

Chung YS, Kim HS, Park KH, Jugder D, Gao T. 2005. Observations of dust-storms in China, Mongolia and associated dust falls in Korea in spring 2003. *Water, Air and Soil Pollution, Focus* **5**: 15–35.

Fang ZY, Zhu FK, Jiang JX, Qian ZA. 1993. *Sandstorm study in China (in Chinese)*. China Meteorological Press: Beijing; 158, 1–2.

Gao T, Liu JT, Yu X, Kang L, Fan YD, Hu YH. 2002. Objective pattern discrimination model for dust storm forecasting. *Meteorological Applications* **9**: 55–62.

Gao T, Xu YF, Bo YH, Yu X. 2006. Synoptic characteristics of dust storms observed in Inner Mongolia and their influence on the downwind area (the Beijing-Tianjin Region). *Meteorological Applications* **13**: 393–403.

Gong SL, Zhang XY, Zhao TL, Zhang XB, Barrie LA, McKendry IG, Zhao CS. 2006. A simulated climatology of Asian dust aerosol and its trans-Pacific transport. Part II: interannual variability and climate connections. *Journal of Climate* **19**: 104–122.

Hu XQ, Lu NM, Niu T, Zhai PM. 2008. Operational retrieval of Asian sand and dust storm from FY-2C geostationary meteorological satellite and its application to real time forecast in Asia. *Atmosphere Chemistry and Physics* **8**: 1649–1659.

Huang M, Peng GB, Zhang JS. 2006. Application of artificial neural networks to the prediction of dust storms in Northwest China. *Global and Planetary change* **52**: 216–224.

Kurosaki Y, Mikami M. 2003. Resent frequent dust events and their relation to surface wind in East Asia. *Geophysical Research Letter* **30**(14): 1736. DOI:10.1029/2003GLO17261.

Liu CM, Young CY, Lee YC. 2006. Influence of Asian dust storms on air quality in Taiwan. *Science of the Total Environment* **368**: 884–897.

Liu HY, Tian YH, Ding D. 2003. Contributions of different land cover types in Otindag Sandy Bashang area of Hebei Province to the material source of sand stormy weather in Beijing. *Chinese Science Bulletin* **48**(17): 1853–1856.

Liu XD, Yin ZY, Zhang XY, Yang XC. 2004. Analyses of the spring dust storm frequency of northern China in relation to antecedent and concurrent wind, precipitation, vegetation, and soil moisture conditions. *Journal of Geophysical Research* **109**(D16210): 1–16.

Miller SD. 2003. A consolidated technique for enhancing desert dust storms with MODIS. *Geophyics Research Letter* **30**(20): ASC 12: 1–4.

Qian WH, Quan LS, Shi SY. 2002. Variations of dust storm in China and its climate control. *Journal of Climate* **15**: 1216–1229.

Shao YP, Yang Y, Wang JJ, Song ZX, Leslie LM, Dong CH, Zhang ZH, Lin ZH, Kanai Y, Yabuki S, Chun YG. 2003. Northeast Asian dust storms: real-time numerical prediction and validation. *Journal of Geophysical Research* **108**(D22): 4691.

Shi PJ, Zhang H, Wang P. 2000. The regional patterns for combating sandification in sandy disaster affected area in China. *Journal of Natural Disaster* **9**(3): 1–7.

Sun JM, Zhang MY, Liu TS. 2001. Spatial and temporal characteristics of dust storms in China and its surrounding regions, 1960–1999: relations to source area and climate. *Journal of Geophysical Research* **106**(D10): 10,325–10,333.

von Storch H, Zwiers FW. 1999. *Statistical Analysis in Climate Research*. Cambridge University Press: Cambridge; 484, 93–94.

Wang YQ, Zhang XY, Gong SL, Zhou CH, Hu XQ, Liu HL, Niu T, Yang YQ. 2008. Surface observation of sand and dust storm in East Asia and its application in CUACE/Dust. *Atmosphere Chemistry and Physics* **8**: 545–553.

Wilks DS. 1995. *Statistical Methods in the Atmospheric Science*. Academic Press, Inc.: New York; 467, 237–238.

Xu M, Chang CP, Fu CB, Robock A, Robinson D, Zhang HM. 2006. Steady decline of East Asian monsoon winds 1969–2000: evidence from the ground measurements of wind speed. *Journal of Geophysical Research* **111**(D24111): 1–8.

Yan HS. 2003. *Climate Changes: Analyses and Forecast (in Chinese)*. China Meteorological Press: Beijing; 246, 241–242.

Yang YQ, Hou Q, Zhou CH, Liu HL, Wang YQ, Niu T. 2008. Sand/dust storm processes in Northeast Asia and associated large-scale circulations. *Atmosphere Chemistry and Physics* **8**: 25–33.

Yasui M, Zhou J, Liu LC. 2005. Vertical profiles of aeolian dust in a desert atmosphere observed using lidar in Shapotou, China. *Journal of Meteorological Society of Japan* **83**(A): 149–171.

Zhang L, Ding YH, Ren GY. 2005a. Variation of dust weather and its climate attribution analysis in northern part of China (in Chinese). *Journal of Applied Meteorological Science* **16**(5): 583–592.

Zhang XY, Wang YQ, Wang D, Gong SL, Arimoto R, Mao LJ, Li J. 2005b. Characterization and sources of regional-scale transported carbonaceous and dust aerosols from different pathways in coastal and sandy land areas of China. *Journal of Geophysical Research* **110**(D15301): 1–13.

Zou XK, Zhai PM. 2004. Relationship between vegetation coverage and spring dust storms over northern China. *Journal of Geophysical Research* **109**(D003104): 1–9.

